

Fringe Field Effects on Transient Characteristics of Nano-Electromechanical (NEM) Nonvolatile Memory Cells

Boram Han and Woo Young Choi

Abstract—The fringe field effects on the transient characteristics of nano-electromechanical (NEM) memory cells have been discussed by using an analytical model. The influence of fringe field becomes stronger as the size of a cell decreases. By using the proposed model, the dependency of NEM memory transient characteristics on cell parameters has been evaluated.

Index Terms—Nano-electromechanical (NEM), fringe field effect, analytical modeling, transient characteristics

I. INTRODUCTION

As the demand for high capacity memory increases, the scaling of flash memory cell is highly required. Accordingly, the downscaling limit of conventional flash memory is near [1]. In order to overcome these limitations, a nano-electromechanical (NEM) nonvolatile memory cell which features high energy efficiency, high program/erase speed and large sensing margin has been proposed [2]. Fig. 1(a) shows the schematic view of a NEM nonvolatile memory cell. It consists of a write word line (WWL), read word line (RWL), bit line (BL), charge-trapped layer and movable beam connected to the BL. L_{beam} means the beam length, t_{beam} means the beam thickness, $t_{\text{ox,eff}}$ means the equivalent oxide thickness of the charge-trapped layer and t_{gap} means the air gap

thickness between the movable beam and charge-trapped layer. Information is stored by beam position: a pulled-down beam means “0” state while a released beam means “1” state.

In order to boost memory capacity and operation speed, NEM memory cells need to be scaled down. However, as cell scaling improves, the effects of fringe field should be considered for more accurate analysis. It is because the influence of fringe field is strong in the case of a small-sized cell. The steady-state characteristics of NEM memory cells have already been discussed in our previous work [3]. Thus, this paper is contributed to the transient characteristics.

II. MODELING METHOD

In order to emulate the transient characteristics of a NEM memory cell, an analytical model using a simple parallel-plate approximation has been used as shown in shown in Fig. 1(b). The governing equation is

$$m \frac{d^2x}{dT^2} + b \frac{dx}{dT} + kx = F_{\text{ext}} \quad (1)$$

where x is the displacement, T is time, m is the effective beam mass [4], b is the damping coefficient, k is the spring constant of the cantilever beam and F_{ext} is the electrostatic force. F_{ext} consists of the electrostatic force induced by the uniform field (F_{uniform}) and by the fringe field (F_{fringe}) [5]. The rest of the parameters are defined as

$$m = 0.4\rho L_{\text{beam}}W_{\text{beam}}t_{\text{beam}} \quad (2)$$

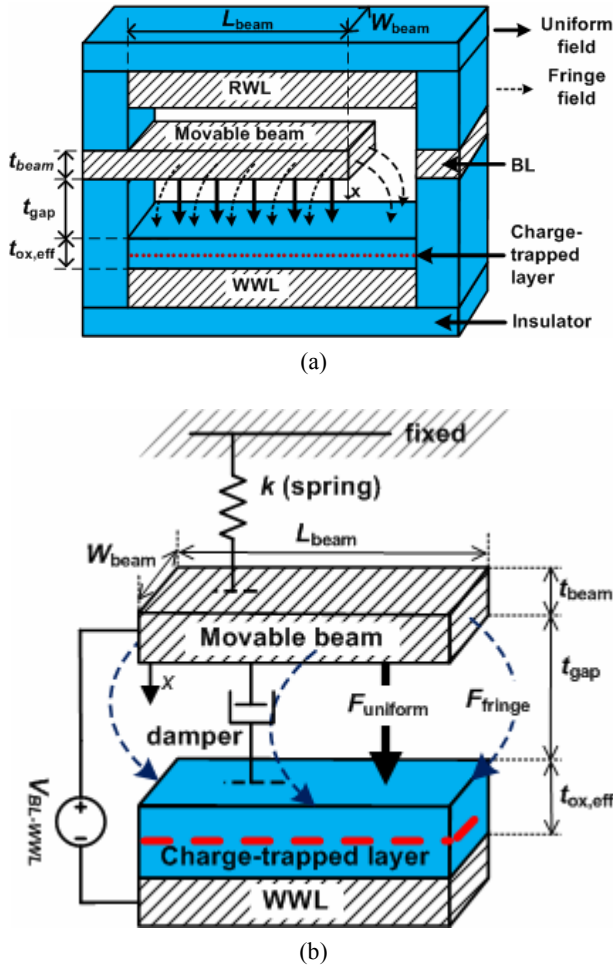


Fig. 1. (a) Schematic of a NEM nonvolatile memory cell, (b) Analytical model of a NEM memory cell under the fringe field effects. Sheet charge is confined within the dashed lines.

$$b = \frac{\sqrt{mk}}{Q} \quad (3)$$

$$k = \frac{2EW_{beam}t_{beam}^3}{3L_{beam}^3} \quad (\text{cantilever beam}) \quad (4)$$

where ρ is the density of the beam material, Q is the beam quality factor and E is the Young's modulus of the beam material. The value of Q was assumed to be 0.5 for critical damping.

From now on, the transient characteristics of a NEM memory cell will be discussed in terms of including pull-in ($T_{pull-in}$), and release time ($T_{release}$). $T_{pull-in}$ is related to the erase speed and $T_{release}$ is related to the program speed. In other words, $T_{pull-in}$ and $T_{release}$ mean erase and program time, respectively. In order to obtain $T_{pull-in}$ and $T_{release}$, time-dependent solutions of (1) have been derived by

using MATLAB [6]. In order to obtain the time-dependent closed-form solutions of (1), two cases can be considered: acceleration-limited or damping-limited case [7]. In the former case when acceleration determines the beam movement due to small b and large Q (> 2), (1) is approximated as below

$$m \frac{d^2x}{dT^2} + kx = F_{ext} \quad (5)$$

In the latter case when damping determines the beam movement due to high b and small Q (≤ 0.5), (1) is approximated as below

$$b \frac{dx}{dT} + kx = F_{ext} \quad (6)$$

Out of the abovementioned two cases, this work focuses on the damping-limited case because NEM memory cells generally have small Q and large damping force [8]. Fig. 2 shows the solution of (1) when Q is equal to 0.5. Once the relationship between x and T is plotted by using MATLAB, each force can be plotted as a function of time. In modeling, V_{BL-WWL} for erase operation is assumed to be $1.5 \times V_{pull-in}$, and V_{BL-WWL} for program operation is assumed to be $0.5 \times V_{release}$. V_{BL-WWL} means the voltage difference between the BL and WWL.

In the first place, $T_{pull-in}$ without the fringe field effects ($T_{pull-in(w/o \text{ fringe})}$) can be calculated. In the case of pull-in operation, initially ($T = 0$), the beam is flat ($x = 0$), which means that the spring force (kx) can be assumed to be zero. Thus, (6) is simplified into

$$b \frac{dx}{dT} = \frac{1}{2} \frac{\epsilon_0 L_{beam} W_{beam} V_{BL-WWL}^2}{(t_{gap} + t_{ox,eff} / \epsilon_r)^2} \quad (7)$$

Then, $T_{pull-in(w/o \text{ fringe})}$ can be obtained by integrating (7). The integration interval is from the initial position ($x = 0$) to the pull-in position ($x = (t_{gap} + t_{ox,eff} / \epsilon_r) / 3$). Thus, $T_{pull-in(w/o \text{ fringe})}$ is

$$T_{pull-in(w/o \text{ fringe})} = \frac{2b(t_{gap} + t_{ox,eff} / \epsilon_r)^3}{3\epsilon_0 L_{beam} W_{beam} V_{BL-WWL}^2} = \frac{3}{2\sqrt{15}} \sqrt{\frac{\rho}{E}} \frac{L_{beam}^2}{t_{beam}} \quad (8)$$

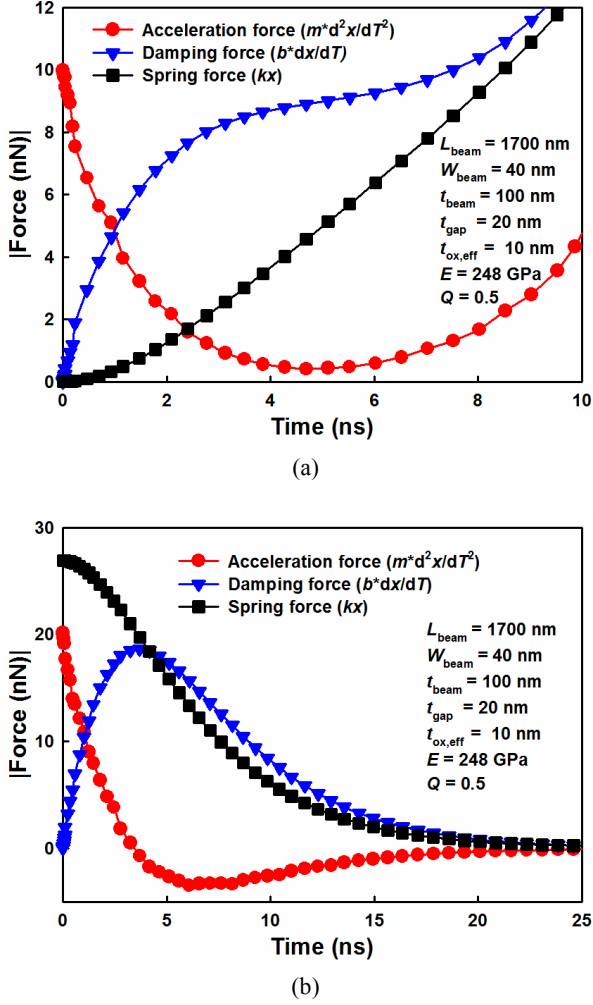


Fig. 2. Comparison of forces (a) in pull-in, (b) release operation.

Second, $T_{\text{pull-in}}$ with fringe field effects ($T_{\text{pull-in(w/ fringe)}}$) can be derived by adding F_{fringe} to the right term of (7). Then, (7) becomes

$$b \frac{dx}{dT} = \frac{\varepsilon_0 L_{\text{beam}} W_{\text{beam}} V_{\text{BL-WWL}}^2}{2(t_{\text{gap}} + t_{\text{ox,eff}} / \varepsilon_r)^2} + \frac{\varepsilon_0 (2L_{\text{beam}} + W_{\text{beam}}) V_{\text{BL-WWL}}^2}{4\pi(t_{\text{gap}} + t_{\text{ox,eff}} / \varepsilon_r)} \quad (9)$$

By integrating (9), $T_{\text{pull-in(w/ fringe)}}$ is derived as

$$T_{\text{pull-in(w/ fringe)}} = \frac{T_{\text{pull-in(w/o fringe)}}}{1 + (1/L_{\text{beam}} + 2/W_{\text{beam}})(t_{\text{gap}} + t_{\text{ox,eff}} / \varepsilon_r) / 2\pi} \quad (10)$$

According to (10), $T_{\text{pull-in(w/ fringe)}}$ is always smaller than $T_{\text{pull-in(w/o fringe)}}$. Also, as fringe field effects become stronger, $T_{\text{pull-in}}$ becomes smaller.

Third, T_{release} without the fringe field effects ($T_{\text{release(w/o fringe)}}$) is calculated. In the case of release operation, initially ($T = 0$), the beam is attached to the charge-trapped layer ($x = t_{\text{gap}}$), which means that the spring force can be assumed to be kt_{gap} . Thus, (6) is simplified into

$$b \frac{dx}{dT} + kt_{\text{gap}} = \frac{1}{2} \frac{\varepsilon_0 L_{\text{beam}} W_{\text{beam}} V_{\text{BL-WWL}}^2}{(t_{\text{ox,eff}} / \varepsilon_r)^2} \quad (11)$$

Then, $T_{\text{release(w/o fringe)}}$ can be obtained by integrating (11). The integration interval of x is from t_{gap} to 0. Thus, $T_{\text{release(w/o fringe)}}$ is

$$T_{\text{release(w/o fringe)}} = \frac{2b(t_{\text{ox,eff}} / \varepsilon_r)^2}{2kt_{\text{gap}}(t_{\text{ox,eff}} / \varepsilon_r)^2 - \varepsilon_0 L_{\text{beam}} W_{\text{beam}} V_{\text{BL-WWL}}^2} = \frac{2}{\sqrt{15}} \sqrt{\frac{\rho}{E}} \frac{L_{\text{beam}}^2}{t_{\text{beam}}} \quad (12)$$

Fourth, T_{release} with fringe field effects can be derived by adding F_{fringe} to the right term of (11). Then, (11) becomes

$$b \frac{dx}{dT} - kt_{\text{gap}} = \frac{\varepsilon_0 L_{\text{beam}} W_{\text{beam}} V_{\text{BL-WWL}}^2}{2(t_{\text{ox,eff}} / \varepsilon_r)^2} + \frac{\varepsilon_0 (2L_{\text{beam}} + W_{\text{beam}}) V_{\text{BL-WWL}}^2}{4\pi(t_{\text{ox,eff}} / \varepsilon_r)} \quad (13)$$

By integrating (13), $T_{\text{release(w/ fringe)}}$ is derived as

$$T_{\text{release(w/ fringe)}} = \frac{T_{\text{release(w/o fringe)}}}{1 - (1/L_{\text{beam}} + 2/W_{\text{beam}})(t_{\text{ox,eff}} / \varepsilon_r) / 6\pi} \quad (14)$$

According to (14), $T_{\text{release(w/ fringe)}}$ is always larger than $T_{\text{release(w/o fringe)}}$. Also, as fringe field effects become stronger, T_{release} becomes larger.

III. SIMULATION RESULTS

In this chapter, the transient characteristics of NEM memory cells depending on cell parameters will be

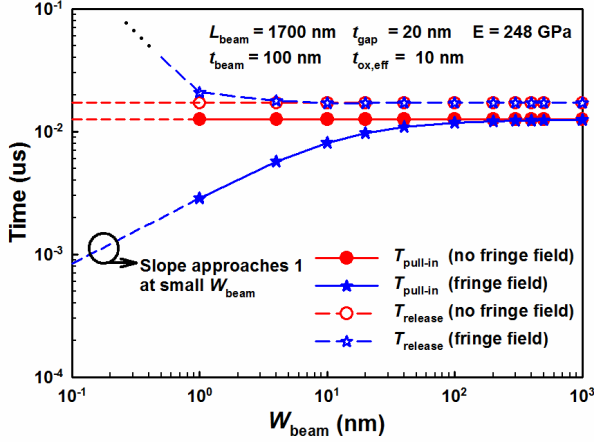


Fig. 3. Transient characteristics as a function of W_{beam} .

discussed in terms of fringe field effects. The simulated reference cell has an L_{beam} of 1700 nm, W_{beam} of 40 nm, t_{beam} of 100 nm, t_{gap} of 30 nm and $t_{ox,eff}$ of 10 nm as shown in Fig. 1. Beam material is assumed to be titanium nitride whose E is 248 GPa and charge-trapped layer material is assumed to be silicon oxide whose ϵ_r is 4.

Fig. 3 shows the transient characteristics depending on W_{beam} with or without fringe field effects. As W_{beam} becomes smaller, the fringe field effects become stronger because the bottom area of a movable beam becomes smaller while the sidewall area of the beam remains constant [3]. Fig. 3 shows that stronger fringe field makes $T_{pull-in}$ smaller and $T_{release}$ larger as predicted in (10) and (14). For example, in the case of carbon nanotubes or nanowires [9], the distinction between the uniform and fringe field is meaningless. If the beam is extremely narrow as below

$$W_{beam} \ll (2/3\pi)(t_{gap} + (t_{ox,eff}/\epsilon_r)), \quad (15)$$

(10) is modified into

$$T_{pull-in(w/fringe)} = \frac{3\pi}{2\sqrt{15}} \sqrt{\frac{\rho}{E}} \frac{L_{beam}^2 W_{beam}}{t_{beam} (t_{gap} + t_{ox,eff}/\epsilon_r)}. \quad (16)$$

According to (16), at extremely small W_{beam} , $d(\log T_{pull-in})/d(\log W_{beam})$ approaches 1 as shown in Fig. 3.

Fig. 4 shows the transient characteristics as a function of L_{beam} . According to (8) and (12), if fringe field effects are ignored, both $d(\log T_{pull-in})/d(\log L_{beam})$ and $d(\log T_{release})/d(\log L_{beam})$ are 2. However, as L_{beam} decreases, the fringe field emitting out of the beam frontwall becomes stronger. Then, $T_{pull-in}$ decreases while $T_{release}$ increases. It is because the beam frontwall area is independent of L_{beam} while the beam bottom and sidewall area become smaller as L_{beam} decreases. Assuming L_{beam} is extremely small as below

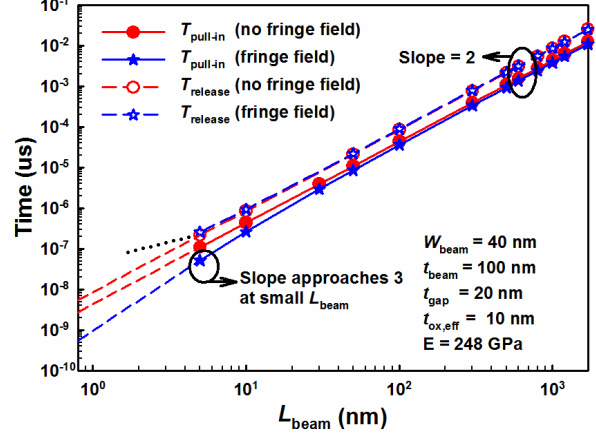


Fig. 4. Transient characteristics as a function of L_{beam} .

$T_{release}/d(\log L_{beam})$ are 2. However, as L_{beam} decreases, the fringe field emitting out of the beam frontwall becomes stronger. Then, $T_{pull-in}$ decreases while $T_{release}$ increases. It is because the beam frontwall area is independent of L_{beam} while the beam bottom and sidewall area become smaller as L_{beam} decreases. Assuming L_{beam} is extremely small as below

$$L_{beam} \ll (t_{gap} + t_{ox,eff}/\epsilon_r)/(3\pi), \quad (17)$$

(10) is rewritten into

$$T_{pull-in(w/fringe)} = \frac{6\pi}{2\sqrt{15}} \sqrt{\frac{\rho}{E}} \frac{L_{beam}^3}{t_{beam} (t_{gap} + t_{ox,eff}/\epsilon_r)} \quad (18)$$

Thus, as L_{beam} becomes smaller, $d(\log T_{pull-in})/d(\log L_{beam})$ approaches 3 as shown in Fig. 4.

Fig. 5 shows the transient characteristics depending on t_{beam} . If fringe field effects are ignored, both $d(\log T_{pull-in})/d(\log L_{beam})$ and $d(\log T_{release})/d(\log L_{beam})$ are -1 as predicted in (8) and (12). Interestingly, in the case of t_{beam} scaling, the inclusion of fringe field effects has no influence on both $d(\log T_{pull-in})/d(\log L_{beam})$ and $d(\log T_{release})/d(\log L_{beam})$. It is because F_{fringe} in (9) and (13) is independent of t_{beam} [3]. The inclusion of fringe field effects leads to 15-% $T_{pull-in}$ reduction and 0.6-% $T_{release}$ increment. It means fringe field effects are stronger in pull-in operation than in release operation.

Fig. 6 shows the transient characteristics as a function of t_{gap} . According to (8) and (12), if fringe field effects

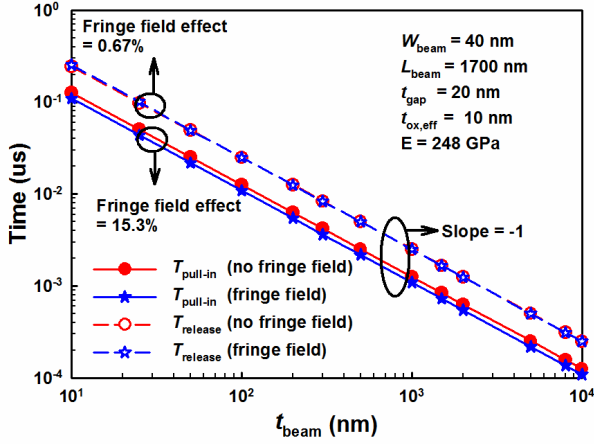


Fig. 5. Transient characteristics as a function of t_{beam} .

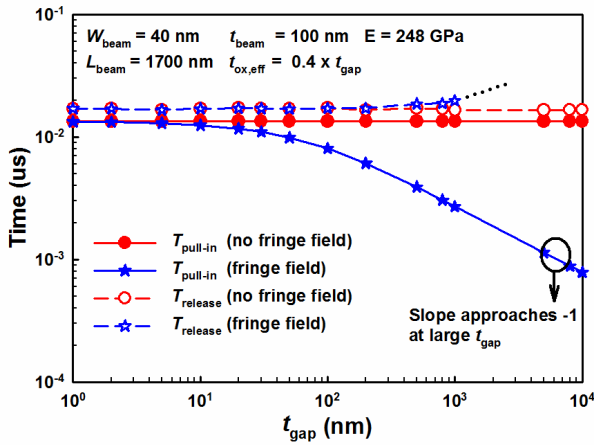


Fig. 6. Transient characteristics as a function of t_{gap} .

are ignored, t_{gap} has no influence on transient characteristics. However, if fringe field effects are included, the increase of t_{gap} makes $T_{pull-in}$ smaller and $T_{release}$ larger. It is because $F_{uniform}$ is more sensitive to the gap between the beam and WWL than F_{fringe} as shown in (9) and (13). If t_{gap} is extremely large as below

$$t_{gap} + \frac{t_{ox,eff}}{\epsilon_r} \gg \frac{3\pi}{1/L_{beam} + 2/W_{beam}}, \quad (19)$$

(10) is rewritten into

$$T_{pull-in(w/ fringe)} = \frac{6\pi}{2\sqrt{15}} \sqrt{\frac{\rho}{E}} \frac{L_{beam}^2}{t_{beam} \left((1/L_{beam}) + (2/W_{beam}) \right) (t_{gap} + t_{ox,eff} / \epsilon_r)} \quad (20)$$

Thus, considering fringe field effects, as t_{gap} becomes larger, $d(\log T_{pull-in})/d(\log t_{gap})$ approaches -1 as shown in Fig. 6.

IV. CONCLUSIONS

The transient characteristics of NEM nonvolatile memory cells have been discussed in terms of fringe field effects. As W_{beam} and L_{beam} decrease or t_{gap} increases, fringe field effects become strong. Based on the analytical model, it has been confirmed that stronger fringe field effects make $T_{pull-in}$ smaller and $T_{release}$ larger, which means faster erase and slower program.

ACKNOWLEDGMENTS

This work was supported in part by the NRF of Korea funded by the MSIP under Grant NRF-2012R1A2A2A01006159 (Mid-Career Researcher Program), in part by the NIPA funded by the MSIP under Grant NIPA-2014-H0301-14-1007 (Information Technology Research Center), in part by the MOTIE/KSRC under Grant 10044842 (Future Semiconductor Device Technology Development Program) and in part by the Sogang University Research Grant of 2014. (e-mail: wchoi@sogang.ac.kr)

REFERENCES

- [1] S. Lai, "Tunnel oxide and ETOXtm flash scaling limitation," *Pro. Nonvolatile Memory Technology Conf.*, pp. 6-7, Jun. 1998.
- [2] W. Y. Choi, H. Kam, D. Lee, J. Lai, and T.-J. King Liu, "Compact nano-electro-mechanical non-volatile memory (NEMory) for 3D integration," *Technical Digest of IEDM*, pp. 603-606, Dec., 2007.
- [3] B. Han and W. Y. Choi, "Analytical model of nano-electromechanical (NEM) nonvolatile memory cells," *IEICE Trans. Electron.*, vol. E95-C, no. 5, pp.914-916, May 2012.
- [4] G. M. Rebeiz, *RF MEMS Theory, Design, and Technology*. Hoboken, NJ: Wiley, 2003.
- [5] R. S. Elliott, *Electromagnetics*, New York: McGraw-Hill, pp. 182-189, 1966.
- [6] MATLAB, 2010, MathWorks Inc. Release 13.
- [7] R. K. Gupta and S. Senturia, "Pull-in time

dynamics as a measure of absolute pressure,” in *IEEE 10th International Conference on Microelectromechanical Systems*, Jan. 1997, pp. 290-294.

- [8] J. Jeon, Ph. D. Thesis, UC Berkeley, 2011.
- [9] U. Ganguly, C. Lee, T.-H. Hou, and E. C. Kan, “Enhanced electrostatics for low-voltage operations in nanocrystal based nanotube/nanowire memories,” *IEEE Trans. Nanotechnol.*, vol. 6, no. 1, pp. 22-28, Jan. 2007.



Boram Han was born in Incheon, in 1988. She received the B.S. and M.S. degrees in the Department of Electronic Engineering from Sogang University, Seoul, Korea, in 2011 and 2013, respectively. Her research interests include the characteristics of

Nano-Electromechanical (NEM) Nonvolatile Memory Cells.



Woo Young Choi was born in Incheon, Korea, in 1978. He received the B.S., M.S. and Ph. D. degrees in the School of Electrical Engineering from Seoul National University, Seoul, Korea in 2000, 2002 and 2006, respectively. From 2006 to 2008, he

was with the Department of Electrical Engineering and Computer Sciences, University of California, Berkeley, USA as a post-doctor. Since 2008, he has been a member of the faculty of Sogang University (Seoul, Korea), where he is currently an Associate Professor with the Department of Electronic Engineering. He has authored or coauthored over 120 papers in international journals and conference proceedings and holds 25 Korean patents. His current research interests include fabrication, modeling, characterization and measurement of CMOS/CMOS-compatible semiconductor devices and nanoelectromechanical (NEM) relays/memory cells.